



Graphitization of amorphous carbon by swift heavy ion impacts: Molecular dynamics simulation

K. Kupka^{a,b}, A.A. Leino^c, W. Ren^c, H. Vázquez^c, E.H. Åhlgren^{d,g}, K. Nordlund^g, M. Tomut^a, C. Trautmann^{a,b}, P. Kluth^e, M. Toulemonde^f, F. Djurabekova^{c,*}

^a GSI Helmholtzzentrum für Schwerionenforschung GmbH, Darmstadt, Germany

^b Technische Universität Darmstadt, Germany

^c Helsinki Institute of Physics and Department of Physics, University of Helsinki, P.O. Box 43, FI-00014, Finland

^d School of Chemistry, University of Nottingham, University Park, Nottingham NG7 2RD, United Kingdom

^e Department of Electronic Materials Engineering, Research School of Physics, Australian National University, Canberra, ACT 2601, Australia

^f CIMAP-GANIL (CEA-CNRS-ESNSICAEN-Univ. Caen) Caen-cedex, France

^g Department of Physics, P.O. Box 43, FI-00014, University of Helsinki, Finland

A B S T R A C T

Stable C-C bonds existing in several *sp* hybridizations place carbon thin films of different structural compositions among the materials most tolerant to radiation damage, for applications in extreme environments. One of such applications, solid state electron stripper foils for heavy-ion accelerators, requires the understanding of the structural changes induced by high-energy ion irradiation. Tolerance of carbon structure to radiation damage, thermal effects and stress waves due to swift heavy ion impacts defines the lifetime and operational efficiency of the foils. In this work, we analyze the consequences of a single swift heavy ion impact on two different amorphous carbon structures by means of molecular dynamic simulations. The structures are constructed by using two different recipes to exclude the correlation of the evolution of *sp*²-to-*sp*³ hybridization with the initial condition. Both initial structures contain approximately 60% of *sp*²-bonded carbon atoms, however, with different degree of clustering of atoms with *sp*³ hybridization. We simulate the swift heavy ion impact employing an instantaneous inelastic thermal spike model. The analysis of changes in density, bonding content and the number and size of carbon primitive rings reveals graphitization of the material within the ion track, with higher degree of disorder in the core and more order in the outer shell. Simulated track dimensions are comparable to those observed in small angle x-ray scattering measurements of evaporation-deposited amorphous carbon stripper foils irradiated by 1.14 GeV U ions.

1. Introduction

Generation of stable beams of highly charged heavy ions for nuclear and material research applications relies on prolonged performance of solid state electron stripping foils. In the course of new developments of accelerator technologies, the materials used for such foils are expected to withstand very high intensity primary beams. The excellent performance of amorphous carbon with respect to beam parameters after electron stripping, such as charge state, and low energy straggling, combined with advantages related to thin film fabrication, low density, excellent thermo-mechanical properties and low activation of beamline components [1,2] bring this material to the top of possible material candidates. Reliably working stripper foils as well as prediction and increase of their lifetime are of great interest and have been thoroughly investigated experimentally [3–11].

On the other hand, atomistic simulations provide complementary information to experiments on material modifications at a smaller scale. Furthermore, experiments usually study ion-induced effects post mortem, whereas simulations follow track formation on the atomic scale right after the energy was deposited by the ions. Carbon-based materials show a huge variety of chemical and physical properties that can be attributed to versatile microstructures. Amorphous carbons consist primarily of atoms with *sp*² and *sp*³ hybridizations. Hereafter for simplicity, the fraction of atoms with *sp*² (or *sp*³) hybridizations will be referred to as the *sp*² (or *sp*³) fraction. The ratio and clustering of these bonding configurations essentially determine the material properties [12,13].

Previous studies on films with a high fraction of *sp*³ hybridization (commonly referred to as tetrahedral amorphous carbon or diamond-

* Corresponding author.

E-mail address: flyura.djurabekova@helsinki.fi (F. Djurabekova).

like carbon) show that the irradiation with swift heavy ions significantly changes the density and bonding content [14–20]. This work concentrates on the effects of swift heavy ion impacts in amorphous carbon films with 60% sp² content.

Simulation cells were produced by liquid quenching and plasma deposition, forming cells with a different degree of clustering. Swift heavy ion impacts by 1.14 GeV U are mimicked by an instantaneous energy deposition calculated from the inelastic thermal spike model [21], similar to the simulation setup used to model track formation in silica [22]. In addition to the investigation of changes in density and bonding content, an analysis of the number and size of carbon rings is presented, providing a deeper insight into structural changes of ion tracks in amorphous carbon. Track dimensions by the simulations are compared with the track radius from small angle x-ray scattering (SAXS) measurements of evaporation-deposited amorphous carbon stripper foils irradiated by 1.14 GeV (4.8 MeV/u) U ions at the linear accelerator UNILAC at GSI (Darmstadt).

2. Computational methods

2.1. Molecular dynamics simulation

Molecular dynamics (MD) simulations offer atomistic insights into structural changes during swift heavy ion irradiation. The movement of atoms is simulated by calculating the force on the atoms from an interatomic potential function. This method enables us to study material modifications induced by swift heavy ions at the atomistic scale. The simulations presented in this paper were performed with the classical MD code PARCAS [23], [24]. Two kinds of simulations were performed: (i) initial sets of simulations to prepare amorphous carbon (carried out in 2 different approaches, as described in detail in Section 2.3), and (ii) a set where the swift heavy ion modification of the obtained structures was simulated. The temperature and pressure of the simulated amorphous carbon preparation were controlled by applying the Berendsen [25] thermostat with the time scaling factor $\tau_T = 50$ fs and barostat with the time constant $\tau_p = 1000$ fs. We also applied the Berendsen temperature control in narrow regions (3 and 4 Å in the DLC films deposition simulations) near the lateral borders of the cell in ion irradiation simulations to minimize the artefacts of temperature control. The empirical Brenner-Beardmore potential [26] as an implementation of the original Brenner potential [27], [28] with extended cut-off parameters ($R = 1.95$ Å, $S = 2.25$ Å) [29] was used for calculation of C-C interactions. Periodic boundaries were applied to simulate bulk material. A time step of 0.26 fs was used for the preparation calculations, ensuring energy conservation in the system. Because some atoms have initially fairly high energies around 10 eV after ion energy deposition, an adaptive time step designed to be able to handle strong collisions was used [30] initially. The maximum time step used at the end of the simulations was the same value of 0.26 fs.

2.2. Analysis of simulation cells

Visualization of the simulation cells was performed with the open visualization tool OVITO [31]. The obtained simulation data was analyzed in terms of temperature, coordination number, density, as well as size and number of carbon rings as a function of radius from the track center.

The temperature was calculated from the velocities of the atoms. We analyzed the coordination environment of every atom within the cut-off of 1.9 Å. This cut-off was chosen at the minimum position between the first and second peak in the pair distribution function. The atoms with coordination number $n \leq 3$ were defined as atoms with sp² hybridization, while atoms with $n \geq 4$ were counted as atoms with sp³ hybridization. Radial analysis of temperature, coordination number and density were performed by dividing the simulation cell into concentric cylindrical shells of equal width. The optimal width, with respect to

obtaining statistically significant results while not losing too much spatial resolution, of each shell was found to be 10 Å. Within each shell, the density $\rho(r)$ was evaluated according to

$$\rho(r) = \frac{Nm_c}{\sum_i V_i} \quad (1)$$

where N is the number of atoms in the shell, m_c the mass of carbon and the denominator describes the sum over atomic volumes V_i within the shell. The atomic volumes were evaluated using the Voro++ library [32].

The track radii were calculated by applying a fitting function to the density distribution in the final frame after the deposited energy was relaxed and the structure was cooled to 300 K. The fitting function has the form of a Fermi distribution where r_t describes the radius of the half-density and is assumed to equal the track radius:

$$f = \frac{\rho_{min} - \rho_0}{\exp\left(\frac{r-r_t}{r_{\rho_0}}\right) + 1} + \rho_0. \quad (2)$$

Here ρ_{min} is the minimum density at the track center, ρ_0 is the bulk density outside the track and r_{ρ_0} denotes the width of the transition from the track density to the bulk density ρ_0 .

To characterize the number and size of the prime carbon rings (rings without a short-cut) [33], the simulation cell was divided into cylindrical shells of 5 Å in width. The number of “shortest rings” (the shortest prime rings for each atom) of a certain length was normalized to the total number of shortest rings in the corresponding shell. Since there is only one shortest ring for each atom, the total number of shortest rings corresponds to the total number of atoms in a certain shell.

2.3. Preparation of amorphous carbon structure

The atomic level structure of amorphous carbon depends on the synthesis method used, both in experiments and simulations. As we shall show later, also the nature of the swift heavy ion modification of this material depends on details of the initial structure. To allow for reproducibility of our results, we hence describe here in detail the two ways in which amorphous carbon was synthesized in the current simulations. Amorphous carbon simulation cells of about 60% sp² fraction were created by two different methods: (i) Quenching from the melt and (ii) plasma deposition. Such structures are comparable to the measured ones for the stripper foils applied in the GSI accelerator and used for the SAXS experiment.

2.3.1. Quenching from melt

Preparation of the amorphous carbon cell by quenching from melt method consisted of several steps: First, carbon atoms were inserted randomly to the initial cell ($20 \times 20 \times 20$ Å³ in size). The number of the atoms needed for 60% sp² amorphous carbon was roughly estimated by a linear interpolation between the densities of graphite and diamond. In the next step, the sample was cooled down from high temperature (2000–6000 K) to 300 K during 100 ps with different cooling rates, searching for the desired sp² fraction and minimum potential energy configuration. Stresses in the cell were allowed to relax by applying the Berendsen pressure control (see Section 2.1).

The best structure was obtained for 1200 atoms, quenched from 5000 to 300 K with a cooling rate of 0.1 K/fs, resulting in a sp² content of 58% (Fig. 1 a)). However, the density of this amorphous carbon sample was approximately 3.0 g/cm³ and therefore slightly higher than the density of 2.7 g/cm³ deduced by linear interpolation. Tensile stresses of about –10 kbar were relaxed by adjusting the cell size. A larger cell of adequate size (1,350,000 atoms, $297.5 \times 299.1 \times 100.2$ Å³) for the ion irradiation was obtained by replication of the small cell over periodic boundaries 5 times in the depth (z) direction and 15 times in the lateral directions. The velocities were randomized by simulating the atom movements at 1000 K followed by slow cooling

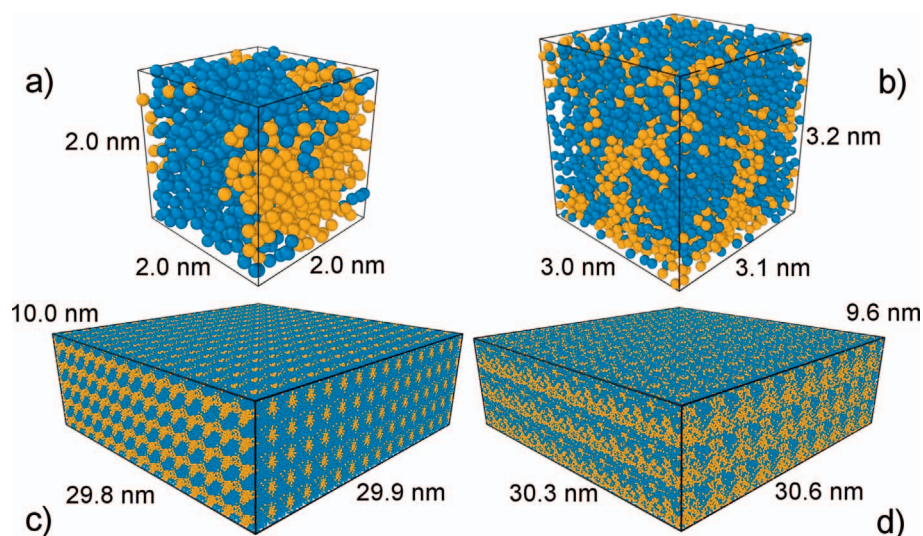


Fig. 1. Seed cells prepared by liquid quenching (a) and plasma deposition (b). Blue colored atoms represent 3-fold coordinated atoms (sp^2) and orange colored atoms are 4-fold coordinated atoms (sp^3). (c) and (d) present the corresponding final large cells for the ion irradiation consisting of multiple cells shown in by the cells in (a) and (b), respectively.

to 300 K. The resulting structure showed inclusions of sp^3 hybridized atoms in a sp^2 matrix as presented in Fig. 1 c). The overall sp^2 content was calculated to remain 58%.

2.3.2. Plasma deposition

In addition to the cell created by the quenching method, two cells were obtained by plasma deposition. In these simulations, the parameters were slightly different from those used for other simulations presented in this publication. The amorphous carbon film was grown on a (111)-oriented diamond substrate of about $30 \times 30 \times 20 \text{ \AA}$ size. The atoms were deposited from normal incidence with an initial energy of 30 eV. Two atomic layers were fixed at the bottom substrate surface to prevent the entire system from moving during the irradiations. Each bombardment was simulated for a time scale of 10 ps, followed by a relaxation time of 3 ps linearly cooling down the entire system to 300 K between subsequent impacts. The analytic bond-order potential of Brenner [28] with extended cut-off parameters was used to model the C-C interactions. By extending the cut-off parameters ($R = 1.95 \text{ \AA}$, $S = 2.25 \text{ \AA}$) a much higher fraction of sp^3 hybridizations could be obtained, as reported by Jaeger and Albe [29]. A small cell with the dimensions $30.29 \times 30.59 \times 32.00 \text{ \AA}^3$ was cut from the inner part of the obtained DLC film. By this, the sp^2 rich surface layer as well as the DLC layer on top of the diamond substrate were removed. This way, we obtained a simulation cell with periodic lateral boundaries, but being non-periodic in the z direction. The simulations of swift heavy ion impacts require periodic conditions in all three dimensions. However, the attempt to apply periodic boundaries on the sides of the new structure will lead to the overlap of positions of atoms on the adjacent sides of the initial cube, causing an artificial burst of potential energy in those positions. In order to avoid this problem, we employed two different methods, which will be denoted as A and B for the sake of clarity. Method A consists of adding an additional empty layer of 1 \AA on top of the simulation cell in z-direction. Subsequently the whole cell is shrunk in this direction to the former height of the cell. Method B consists instead of removing the atoms with a distance to a neighboring atom shorter than 1.1 \AA . In both methods the resulting structures were then heated to 1000 K and subsequently cooled down to 300 K with the rate of 0.1 K/fs . The resulting

cells showed a more homogeneous distribution of atoms with sp^3 hybridization in comparison to the structure obtained by quenching from the melt (Fig. 1 b)). The overall sp^2 fraction was calculated to be 60% for both structures. The cells for the irradiation simulations (size $302.9 \times 305.9 \times 96.0 \text{ \AA}^3$, 1,333,800 atoms for method A (Fig. 1 d)) and 1,331,100 atoms for method B) were obtained by multiplication of the small cells and randomization of velocities by simulating the atom movements at 1000 K and slowly cooling to 300 K (0.1 K/fs). The density of both structures was calculated to be 3 g/cm^3 with a similar distribution of sp^3 hybridized atoms in the sp^2 matrix. All cells were checked for having an adequate size, i.e. allowing heat and pressure wave dissipation. For each method, three different seeds were used to allow for statistical variation, however, the produced results were identical within the accuracy of the analysis method. In the following, the results obtained for the plasma deposited amorphous carbon will be given only for the cell obtained with method A. The results for the cell prepared with method B are very similar and hence are not shown.

To mimic the effect of swift heavy ions, random velocities are given to the atoms at the beginning of the simulation in accordance with the radial kinetic energy distribution profile for 1.14 GeV (4.8 MeV/u) U that was calculated using the inelastic thermal spike (i-TS) model [21] (Fig. 3 b). The i-TS model is a widely used phenomenological model that consists of a coupled set of heat diffusion equations, describing model heat transport in the electronic and atomic subsystems. The kinetic energy profile used in MD simulations corresponds to the temperature profile in the atomic subsystem at about 20 fs, when the temperature of the atomic system has reached the maximum in the i-TS calculation. A value of $10^{13} \text{ J/(sKcm}^3)$ was used as the electron-phonon coupling constant, based on the heat conductivity of graphite (see Toulemonde et al. [34]). The initial temperature before the ion impacts was 300 K.

3. Experimental methods

3.1. Material and swift heavy ion irradiation

20 \mu g/cm^2 amorphous carbon foils produced by resistance

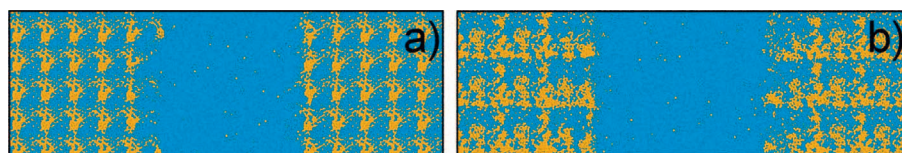


Fig. 2. Cross section of final simulation cells prepared by liquid quenching (a) and plasma deposition (b) after swift heavy ion impact. Ion tracks are visible in the center of the cells visible by the increase of sp^2 bonded atoms (blue). Orange colored atoms correspond to 4-fold coordinated atoms (sp^3).

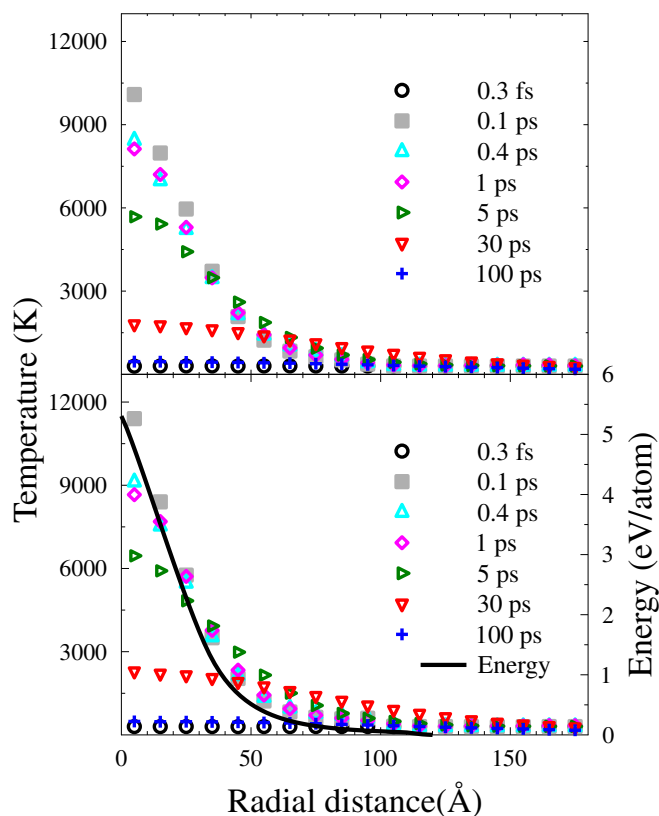


Fig. 3. Time evolution of the temperature increase by a swift heavy ion impact on the quenched (a) and the plasma deposited (b) cell as a function of radial distance from track center. The kinetic energy deposition profile for 1.14 GeV (4.8 MeV/u) U ion is included in figure b with a separate axis.

evaporation under high vacuum at the GSI target laboratory [35] with an initial sp^2 fraction of 60% (as determined by x-ray photoelectron measurements) were irradiated at the M3-beamline of the linear accelerator UNILAC at GSI (Darmstadt) with 1.14 GeV (4.8 MeV/u) U ions. The irradiation was performed at room temperature under normal beam incidence, achieving a fluence of 1.5×10^{11} ions/cm² with an estimated fluence uncertainty of 10–20 %.

3.2. Small angle x-ray scattering

Small angle x-ray scattering (SAXS) was used to study the tracks formed by the ion irradiation. The experiment was performed at the SAXS/WAXS beamline at the Australian Synchrotron in Melbourne, Australia, using an x-ray energy of 11 keV and 0.04 mm² spot size. Measurements were conducted in transmission mode, with the tracks tilted 5° with respect to the x-ray beam. Scattering from pristine samples was subtracted from the measured spectra. The scattering intensity was analyzed as a function of the scattering vector q and fitted with a cylinder model with constant density to obtain the track radius. Detailed descriptions of the method can be found in publications by Kluth et al. [22,36].

4. Results and discussion

Cross sections of the final simulation cells after the ion impact are presented in Fig. 2. The formation of a track in the center of the simulation cells is well visible by the increase of sp^2 bonded atoms (blue).

The time evolution of the temperature as a function of radial distance from the track center for both quenched and plasma deposited cells is shown in Fig. 3. Immediately after energy deposition (0.1 ps), a rapid temperature increase in the modified region ($r \sim 5$ nm) is

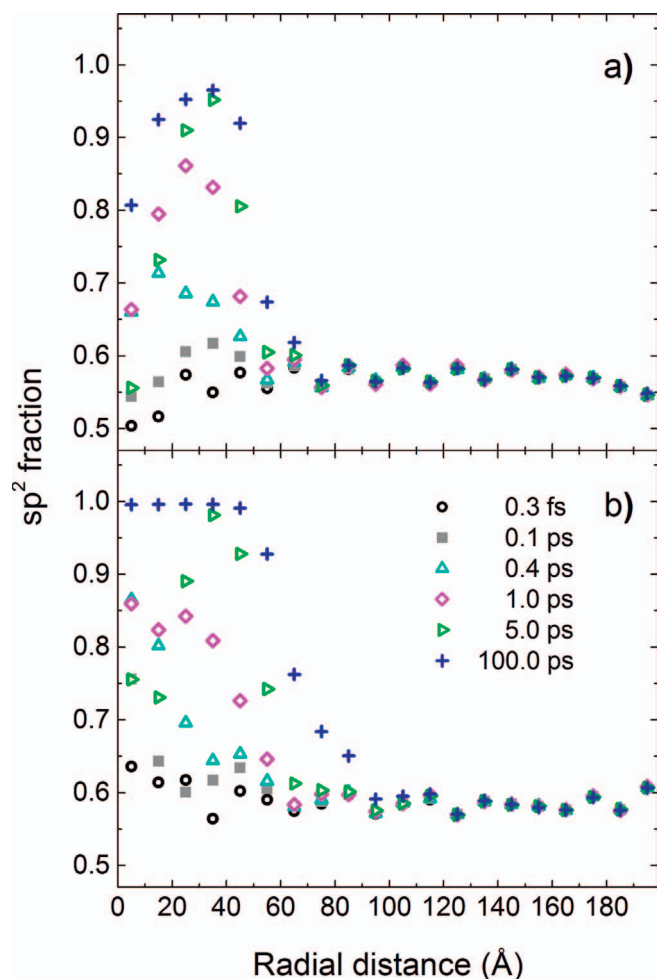


Fig. 4. Time evolution of the sp^2 content as a function of the radial distance from the track center in the quenched (a) and the plasma deposited (b) cell.

observed. The liquid quenched cell (Fig. 3 a) reaches temperatures over 6000 K, while in the plasma deposited cell temperatures few hundred Kelvins higher (Fig. 3 b) are observed. The temperature decreases radially from the track center, reaching ≈ 800 K at the borders of the simulation cells. Since this temperature is considerably below the melting point of carbon (estimated from simulation of carbon[37] with the same potential to be above 3000 K), we assume that the simulation cell is of adequate size for studying the ion impact. Throughout the simulation, the temperature decreases until reaching the initial temperature (300 K) at the end of the simulation (100 ps) for all cells.

Atoms are classified as sp^2 or sp^3 bonded based on their coordination number (3 for sp^2 and 4 for sp^3). In Fig. 4 is shown the sp^2 content with radial distance from the track center. The sp^2 fraction in the track core ($r \sim 5$ nm) increases gradually with simulation time, the maximum values for both cells are reached at the end of the simulations (after 100 ps). At the end of the simulation, the fraction value in the quenched cell varies from 96% to 80% towards the origin while in the plasma cell the value stays uniform. This graphitization is confined to a region of about 50 Å radial distance from the track center. Outside this area, the sp^2 fraction is at the initial level of 60%. The density profiles presented in Fig. 5 show a rapid expansion of the material in the track after energy deposition resulting in a non-equilibrium underdense structure of about 2.2 g/cm³ for the quenched cell and 2.3 g/cm³ for the plasma deposited cell. Relaxation towards the end of the simulation forms a structure of 2.7 and 2.8 g/cm³ density in the track, respectively. The density fluctuation outside the track is due to the segregation of 4-fold coordinated atoms and is therefore stronger for the quenched cell. The

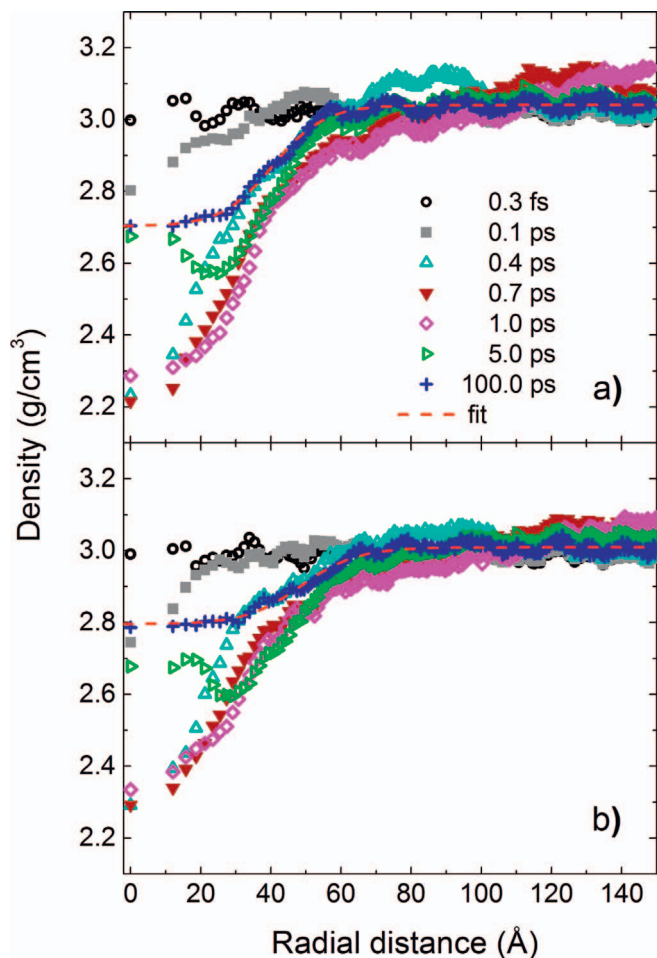


Fig. 5. Time evolution of the density as a function of the radial distance from the track center in the quenched (a) and the plasma deposited (b) cell.

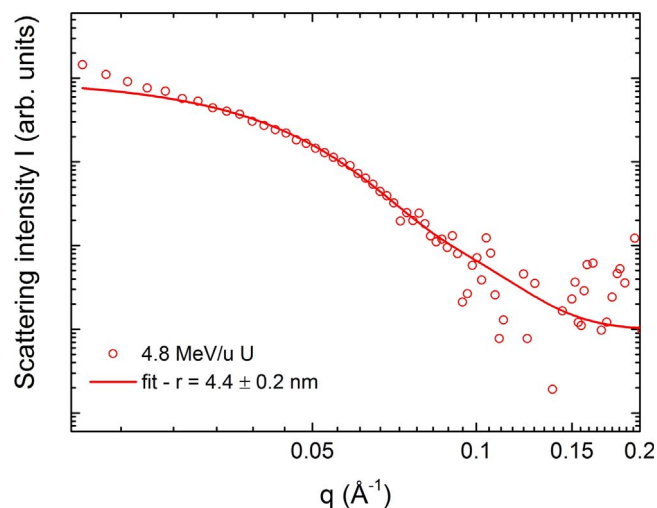


Fig. 6. SAXS pattern as a function of q for amorphous carbon irradiated by 1.14 GeV (4.8 MeV/u) U ions and a fluence of 1.5×10^{11} ions/cm² (open circles) and the corresponding fit to a cylinder model (solid line).

track radii were calculated by fitting a Fermi function to the density data of the relaxed simulation cell after 100 ps (fit shown in Fig. 5) yielding a track radius of 40.5 ± 0.5 Å for the quenched cell and 48.6 ± 0.7 Å for the plasma deposited cell. These track radii can be compared to the experimental values obtained from the SAXS

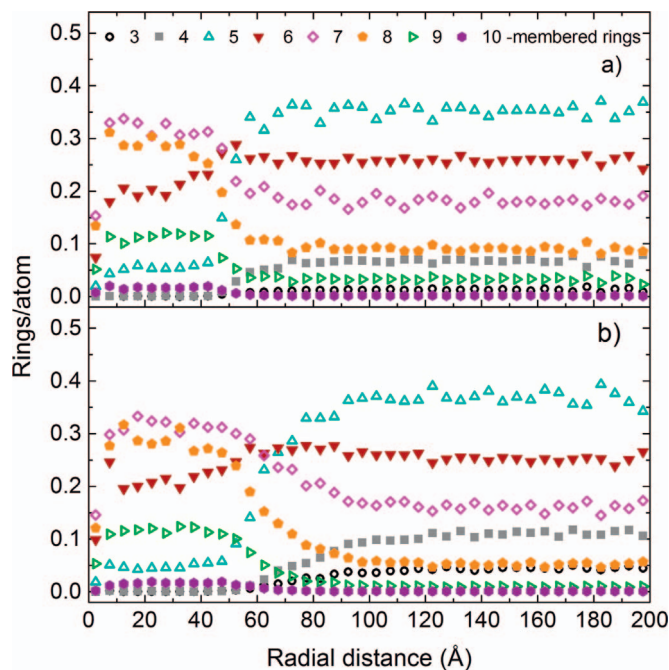


Fig. 7. Rings per atom as a function of radial distance from track center for the relaxed (100 ps) quenched (a) and plasma deposited (b) cell. The term ‘rings per atom’ denotes to the number of shortest rings of a certain size normalized to the total number of shortest rings (atoms) in the corresponding shell.

measurements. Fig. 6 presents the scattering intensity I as a function of scattering value q (open circles) with the corresponding fit by a cylinder model (solid line). The obtained track radius of 44 ± 2 Å lies in between the track radii deduced from the simulations of differently prepared amorphous carbon cells.

High sp^2 content shows graphitization, however further analysis is needed to determine if it is order or disordered graphite. Ring analysis is an efficient method to distinguish between both structures. Ring analysis for the relaxed simulation cell (100 ps) is presented in Fig. 7. For both quenched and plasma deposited cells, the number of rings per atom for ring sizes smaller than six decreases in the area of the track, whereas the number of rings per atom increases for the 7-membered rings or larger. The ratio of the rings per atom of the final relaxed cell and the cell before energy deposition for the 6- and 8-membered rings is presented in Fig. 8 a and b, respectively. The 6-membered rings are abundant in graphite and diamond, whereas 8-membered rings are specific to the graphite structure (di-vacancies), but not in diamond. The decreased number of the 6-membered rings in the core of the track and a slight increase of this number in the outer part of the track constitute a core-shell structure of the track with a disordered core and a more ordered shell region. An increase of the 8-membered rings confirms graphitization, or more precisely, the formation of a damaged graphitic structure in the track, since no 8-membered rings are expected in defected diamond. This is in good accordance with positron annihilation experiments on pristine and swift heavy ion-irradiated highly ordered pyrolytic graphite (HOPG) which show the presence of twofold to fourfold (chain) vacancy clusters [38].

5. Conclusion

Swift heavy ion impacts (1.14-GeV U) on amorphous carbon structures with about 60% sp^2 fraction and a density of 3 g/cm³ were studied by molecular dynamics simulations. During the irradiation simulation the evolution of temperature, sp^2 fraction, density, as well as the size and number of carbon rings are analyzed as a function of radius from the track center. The initial energy deposition was taken into account

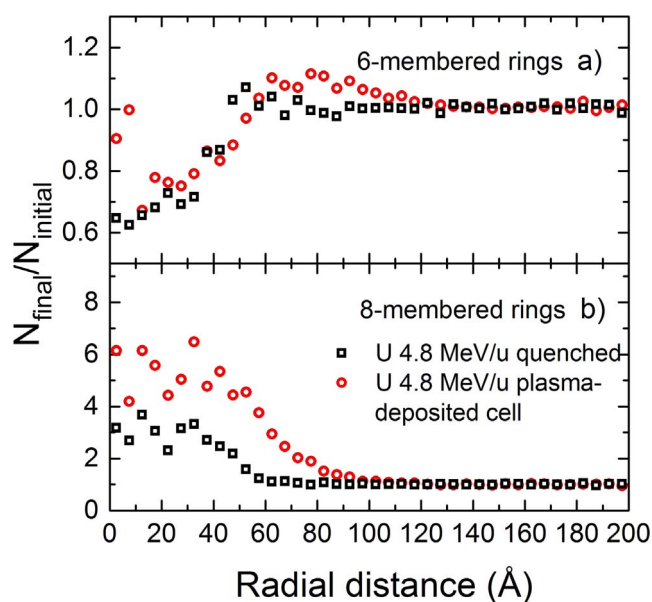


Fig. 8. The change in the number of occurrences of 6-membered (a) and 8-membered (b) rings per atom as a function of radial distance from the track center. The value is given as the ratio of occurrences in the final simulation frame N_{final} to the initial frame $N_{initial}$ and calculated using 3 different simulation cells (cell fabrication methods are given in the legend).

by the inelastic thermal spike model. The present work demonstrates that the Brenner-Beardmore potential is suitable for modeling swift heavy ion impacts. Our results show a graphitization of the amorphous carbon within a cylinder radius of about 5 nm (see Fig. 4) in agreement with other simulations on tetragonal amorphous carbon [14] and experiments [17–20]. The graphitization is characterized by the increase of the sp^2 fraction and a density decrease in the track. In addition, the ring analysis provides evidence of a core-shell structure in the form of a decreased number of the 6-membered rings in the core of the track and a slight increase in the outer part of the track. In the track core, an increase of the 8-membered rings is associated with the formation of a damaged graphitic structure. This finding is in good accordance with positron annihilation experiments on HOPG which show the presence of vacancy clusters [38]. Simulated track dimensions agree well with the experimentally observed track radius in an evaporation-deposited amorphous carbon stripper foil.

Acknowledgments

Katharina Kupka gratefully acknowledges support by BMBF (contract no. 05P12RDRBL) and HGS-HiRe Graduate School. W.R., H.V. and K.N. acknowledge funding from the Academy of Finland project HISCON. We also thank the CSC-IT Center for Science Ltd for the generous grants of computer time. PK acknowledges the Australian Research Council for financial support. Part of this research was undertaken on the SAXS/WAXS beamline at the Australian Synchrotron.

References

- [1] W. Barth, M.S. Kaiser, B. Lommel, M. Maier, S. Mickat, B. Schlitt, J. Steiner, M. Tomut, H. Vormann, Carbon stripper foils for high current heavy ion operation, *J. Radioanal. Nucl. Chem.* 299 (2) (2014) 1047–1053, <http://dx.doi.org/10.1007/s10967-013-2651-3>.
- [2] W. Barth, G. Clemente, L. Dahl, P. Gerhard, L. Groening, B. Lommel, M.S. Kaiser, M. Maier, S. Mickat, W. Vinzenz, H. Vormann (Eds.), *High current design U40+ operation in the GSI-UNILAC*, vol. MOP044, 2010 of LINAC2010.
- [3] H. Okuno, N. Fukunishi, H. Hasebe, H. Imao, O. Kamigaito, M. Kase, H. Kuboki, Charge strippers for radioisotope beam factory at RIKEN, *J. Radioanal. Nucl. Chem.* 299 (2) (2014) 945–949, <http://dx.doi.org/10.1007/s10967-013-2715-4>.
- [4] H. Hasebe, H. Kuboki, H. Okuno, I. Yamane, H. Imao, N. Fukunishi, M. Kase, O. Kamigaito, Development of a new foil compounded from carbon nanotubes and sputter-deposition carbon, *J. Radioanal. Nucl. Chem.* 299 (2) (2014) 1013–1018, <http://dx.doi.org/10.1007/s10967-013-2635-3>.
- [5] H. Hasebe, H. Okuno, H. Kuboki, H. Ryuto, N. Fukunishi, O. Kamigaito, A. Goto, M. Kase, Y. Yano, Development of long-life carbon stripper foils for uranium ion beams, *Nucl. Instrum. Methods Phys. Res., Sect. A* 613 (3) (2010) 453–456, <http://dx.doi.org/10.1016/j.nima.2009.10.002>.
- [6] H. Kuboki, H. Okuno, H. Hasebe, S. Yokouchi, N. Fukunishi, Y. Higurashi, J. Ohnishi, T. Nakagawa, H. Imao, O. Kamigaito, A. Goto, M. Kase, Y. Yano, Charge-state distribution of U238 in nitrogen gas and carbon foil at 14 and 15 MeV/nucleon, *Phys. Rev. Spec. Top. Accel. Beams* 14 (5) (2011), <http://dx.doi.org/10.1103/PhysRevSTAB.14.053502>.
- [7] F. Marti, *Heavy ion strippers, LINAC2012, Vol. FR1A01 2012*, pp. 1050–1054.
- [8] F. Marti, A. Hershcovitch, Y. Momozaki, J. Nolen, C. Reed, P. Thieberger, Development of stripper options for FRIB, linear accelerator conference LINAC2010, 2010, pp. 622–664.
- [9] F. Marti, S. Hitchcock, P. Miller, J.W. Stetson, J. Yurkon, Stripper foil developments at NSCL/MSU, vol. THM2CC003, 2010, pp. 373–375.
- [10] G. Dollinger, P. Maier-Komor, Structure studies of carbon foils with the aim to improve the ability for heavy-ion stripping, *Nucl. Instrum. Methods Phys. Res., Sect. A* 257 (1) (1987) 64–68, [http://dx.doi.org/10.1016/0168-9002\(87\)91179-X](http://dx.doi.org/10.1016/0168-9002(87)91179-X).
- [11] G. Dollinger, P. Maier-Komor, Heavy-ion irradiation damage in carbon stripper foils, *Nucl. Instrum. Methods Phys. Res., Sect. A* 282 (1) (1989) 223–235, [http://dx.doi.org/10.1016/0168-9002\(89\)90145-9](http://dx.doi.org/10.1016/0168-9002(89)90145-9).
- [12] J. Robertson, Diamond-like amorphous carbon, *Mater. Sci. Eng. R. Rep.* 37 (4-6) (2002) 129–281, [http://dx.doi.org/10.1016/S0927-796X\(02\)00005-0](http://dx.doi.org/10.1016/S0927-796X(02)00005-0).
- [13] J. Robertson, Amorphous carbon, *Adv. Phys.* 35 (4) (1986) 317–374, <http://dx.doi.org/10.1080/00018738600101911>.
- [14] D. Schwen, E. Bringa, J. Krauser, A. Weidinger, C. Trautmann, H. Hofsaess, Nanohillock formation in diamond-like carbon induced by swift heavy projectiles in the electronic stopping regime: experiments and atomistic simulations, *Appl. Phys. Lett.* 101 (11) (2012) 113115, <http://dx.doi.org/10.1063/1.4752455>.
- [15] D. Schwen, C. Ronning, H. Hofsaess, Field emission studies on swift heavy ion irradiated tetrahedral amorphous carbon, *Diam. Relat. Mater.* 13 (4-8) (2004) 1032–1036, <http://dx.doi.org/10.1016/j.diamond.2003.11.039>.
- [16] D. Schwen, E. Bringa, Atomistic simulations of swift ion tracks in diamond and graphite, *Nucl. Inst. Methods Phys. Res. B* 256 (1) (2007) 187–192, <http://dx.doi.org/10.1016/j.nimb.2006.12.001>.
- [17] J.-H. Zollondz, D. Schwen, A.-K. Nix, C. Trautmann, J. Berthold, J. Krauser, H. Hofsaess, Conductive nanoscopic ion-tracks in diamond-like-carbon, *Mater. Sci. Eng. C* 26 (5-7) (2006) 1171–1174, <http://dx.doi.org/10.1016/j.msec.2005.09.107>.
- [18] J.-H. Zollondz, J. Krauser, A. Weidinger, C. Trautmann, D. Schwen, C. Ronning, H. Hofsaess, B. Schultrich, Conductivity of ion tracks in diamond-like carbon films, *Diam. Relat. Mater.* 12 (3-7) (2003) 938–941, [http://dx.doi.org/10.1016/S0925-9635\(02\)00339-4](http://dx.doi.org/10.1016/S0925-9635(02)00339-4).
- [19] J. Krauser, J.-H. Zollondz, A. Weidinger, C. Trautmann, Conductivity of nanometer-sized ion tracks in diamond-like carbon films, *J. Appl. Phys.* 94 (3) (2003) 1959, <http://dx.doi.org/10.1063/1.1587263>.
- [20] M. Waiblinger, C. Sommerhalter, B. Pietzak, J. Krauser, B. Mertesacker, M. Lux-Steiner, S. Klauwünzer, A. Weidinger, C. Ronning, H. Hofsaess, Electrically conducting ion tracks in diamond-like carbon films for field emission, *Appl. Phys. A Mater. Sci. Process.* 69 (2) (1999) 239–240, <http://dx.doi.org/10.1007/s003390050996>.
- [21] Z.G. Wang, C. Dufour, E. Paumier, M. Toulemonde, The S e sensitivity of metals under swift-heavy-ion irradiation: a transient thermal process, *J. Phys. Condens. Matter* 6 (34) (1994) 6733–6750, <http://dx.doi.org/10.1088/0953-8984/6/34/006>.
- [22] P. Kluth, C.S. Schnorr, O.H. Pakarinen, F. Djurabekova, D.J. Sprouster, R. Giulian, M.C. Ridgway, A.P. Byrne, C. Trautmann, D.J. Cookson, K. Nordlund, M. Toulemonde, Fine structure in swift heavy ion tracks in amorphous SiO₂, *Phys. Rev. Lett.* 101 (17) (2008), <http://dx.doi.org/10.1103/PhysRevLett.101.175503>.
- [23] K. Nordlund, M. Ghaly, R.S. Averback, M. Caturla, T. Diaz de la Rubia, J. Tarus, Defect production in collision cascades in elemental semiconductors and fcc metals, *Phys. Rev. B* 57 (13) (1998) 7556–7570, <http://dx.doi.org/10.1103/PhysRevB.57.7556>.
- [24] M. Ghaly, K. Nordlund, R.S. Averback, Molecular dynamics investigations of surface damage produced by kiloelectronvolt self-bombardment of solids, *Philos. Mag.* A 79 (4) (1999) 795–820, <http://dx.doi.org/10.1080/01418619908210332>.
- [25] H.J.C. Berendsen, J.P.M. Postma, W.F. van Gunsteren, A. DiNola, J.R. Haak, Molecular dynamics with coupling to an external bath, *J. Chem. Phys.* 81 (8) (1984) 3684, <http://dx.doi.org/10.1063/1.448118>.
- [26] K. Beardmore, R. Smith, Empirical potentials for C[snbd]Si[snbd]H systems with application to C 60 interactions with Si crystal surfaces, *Philos. Mag.* A 74 (6) (1996) 1439–1466, <http://dx.doi.org/10.1080/01418619608240734>.
- [27] D.W. Brenner, Empirical potential for hydrocarbons for use in simulating the chemical vapor deposition of diamond films, *Phys. Rev. B* 42 (15) (1990) 9458–9471, <http://dx.doi.org/10.1103/PhysRevB.42.9458>.
- [28] D.W. Brenner, Erratum: Empirical potential for hydrocarbons for use in simulating the chemical vapor deposition of diamond films, *Phys. Rev. B* 46 (3) (1992) 1948, <http://dx.doi.org/10.1103/PhysRevB.46.1948.2>.
- [29] H.U. Jäger, K. Albe, Molecular-dynamics simulations of steady-state growth of ion-deposited tetrahedral amorphous carbon films, *J. Appl. Phys.* 88 (2) (2000) 1129, <http://dx.doi.org/10.1063/1.373787>.
- [30] K. Nordlund, Molecular dynamics simulation of ion ranges in the 1–100 keV energy range, *Comput. Mater. Sci.* 3 (4) (1995) 448–456, [http://dx.doi.org/10.1016/0927-0256\(94\)00085-Q](http://dx.doi.org/10.1016/0927-0256(94)00085-Q).
- [31] A. Stukowski, Visualization and analysis of atomistic simulation data with OVITO-

- the open visualization tool, *Model. Simul. Mater. Sci. Eng.* 18 (1) (2010) 15012, <http://dx.doi.org/10.1088/0965-0393/18/1/015012>.
- [32] C.H. Rycroft, VORO++: a three-dimensional voronoi cell library in C++, *Chaos (Woodbury, N.Y.)* 19 (4) (2009) 41111, <http://dx.doi.org/10.1063/1.3215722>.
- [33] X. Yuan, A.N. Cormack, Efficient algorithm for primitive ring statistics in topological networks, *Comput. Mater. Sci.* 24 (3) (2002) 343–360, [http://dx.doi.org/10.1016/S0927-0256\(01\)00256-7](http://dx.doi.org/10.1016/S0927-0256(01)00256-7).
- [34] M. Toulemonde, W. Assmann, C. Dufour, A. Meftah, C. Trautmann, Nanometric transformation of the matter by short and intense electronic excitation: experimental data versus inelastic thermal spike model, *Nucl. Instrum. Methods Phys. Res., Sect. B* 277 (2012) 28–39, <http://dx.doi.org/10.1016/j.nimb.2011.12.045>.
- [35] B. Lommel, W. Hartmann, B. Kindler, J. Klemm, J. Steiner, Preparation of self-supporting carbon thin films, *Nucl. Instrum. Methods Phys. Res., Sect. A* 480 (1) (2002) 199–203, [http://dx.doi.org/10.1016/S0168-9002\(01\)02100-3](http://dx.doi.org/10.1016/S0168-9002(01)02100-3).
- [36] D. Schauries, A.A. Leino, B. Afra, M.D. Rodriguez, F. Djurabekova, K. Nordlund, N. Kirby, C. Trautmann, P. Kluth, Orientation dependent annealing kinetics of ion tracks in c-SiO₂, *J. Appl. Phys.* 118 (22) (2015) 224305, <http://dx.doi.org/10.1063/1.4936601>.
- [37] J.N. Glosli, F.H. Ree, The melting line of diamond determined via atomistic computer simulations, *J. Chem. Phys.* 110 (1) (1999) 441, <http://dx.doi.org/10.1063/1.478103>.
- [38] M. Krause, W. Egger, W. Ensinger, C. Hugenschmidt, B. Löwe, L. Ravelli, M. Tomut, C. Trautmann, Positron annihilation lifetime spectroscopy study of vacancy cluster evolution in swift heavy ion irradiated HOPG, GSI SCIENTIFIC REPORT, Vol. 2011-1 2010, p. 384.